



Electrocatalytic activity of Basolite™ F300 metal-organic-framework structures

K. Firoz Babu ^a, M. Anbu Kulandainathan ^a, Ioannis Katsounaros ^b, Liza Rassaei ^c, Andrew D. Burrows ^c, Paul R. Raithby ^c, Frank Marken ^{c,*}

^a Electro-organic Division, Central Electrochemical Research Institute, Karaikudi-630 006, India

^b Aristotle University Thessaloniki, Department of Chemical Engineering, Inorganic Chemistry Laboratory, Thessaloniki 54124, Greece

^c Department of Chemistry, University of Bath, Claverton Down, Bath BA2 7AY, UK

ARTICLE INFO

Article history:

Received 5 February 2010

Received in revised form 17 February 2010

Accepted 17 February 2010

Available online 1 March 2010

Keywords:

MOF

Voltammetry

Prussian blue

Reductive dissolution

Host guest electrochemistry

Water splitting

Sensor

ABSTRACT

For the case of the commercially available metal-organic framework (MOF) structure Basolite™ F300 or Fe (BTC) with BTC = benzene-1,3,5-tricarboxylate, it is shown that the Fe(III/II) electrochemistry is dominated by reductive dissolution rather than ion insertion (which in marked contrast is dominating the behaviour of Fe(III/II) open framework processes in Prussian blues). Solid Fe(BTC) immobilised onto graphite or platinum working electrodes is investigated and it is shown that well-defined and reversible Fe(III/II) reduction responses occur only on platinum and in the presence of aqueous acid. The process is shown to follow a CE-type mechanism involving liberation of Fe(III) in acidic media, in particular for high concentrations of acid. Effective electrocatalysis for the oxidation of hydroxide to O₂ (anodic water splitting) is observed in alkaline aqueous media after initial cycling of the potential into the reduction potential zone. A mechanism based on a MOF-surface confined hydrous iron oxide film is proposed.

© 2010 Elsevier B.V. All rights reserved.

1. Introduction

A lot of recent development has focused on designer porous materials such as metal-organic frameworks or MOFs [1–5]. These materials consist of metal cations bridged by organic ligands in a well-defined three-dimensional structure with nano-sized pores [6]. A wide range of potential building blocks and post-synthesis modification [7,8] open up a vast array of structures and functionalities [9,10].

Pioneering work on the electrochemistry of MOFs has been reported by Doménech-Carbó et al. [11]. For the case of Cu and Zn MOFs with BTC (= benzene-1,3,5-tricarboxylate) ligands, a range of processes including reductive cation insertion, metal nucleation, and partial dissolution have been reported [12]. In situ electrochemical AFM measurements were reported showing interesting metal structures, which grow upon conversion of the MOF to metal nuclei [13]. However, apart from these studies there is only very little information about the electrochemical reactivity of MOF systems [14,15]. The reactivity of porous metal compounds is of considerable interest due to their potential application for electrocatalytic processes and in sensor applications. A considerable body of work exists, for example, on porous Prussian blues [16] which are known to act as versatile electrocatalysts and ion insertion electrodes [17]. It is therefore important to develop new classes of porous solids with electrochemical reactivity and the family of MOF materials appears

uniquely suited based on their structural diversity and known absorption properties [18].

Here, the commercially available Fe(BTC) MOF (Basolite™ F300) with BTC = benzene-1,3,5-tricarboxylate) is investigated. Structurally and electrochemically, this material may be compared with recently synthesised iron-BTC MOFs [19,20] and iron-trimellitates [21], and also with the corresponding Cu and Zn MOFs [11]. A further interesting comparison is possible with the well-known iron-based Prussian blue materials with cyanide bridging ligands. Prussian blue has found many applications and due to facile cation insertion and expulsion processes it has been studied intensely [22]. It is shown here that Fe(BTC) in contrast to Prussian blue does not allow facile cation insertion and that the electrochemical processes of the solid immersed in aqueous electrolyte media are dominated instead by the reductive dissolution (in acidic media) and reductive transformation (in alkaline media).

2. Experimental

2.1. Chemical reagents

All reagents used were of analytical grade purity. Ferric benzene-1,3,5-tricarboxylate, Fe(BTC), was obtained from Aldrich (Basolite™ F300, hydrophilic MOF, re-activation at 200 °C, BET surface area 1300–1600 m² g⁻¹, bulk density 0.16–0.35 g cm⁻³, XRD - amorphous). Hydrochloric acid, potassium chloride, sodium hydroxide, and nitric acid were purchased from Aldrich. Demineralised and filtered water

* Corresponding author. Tel.: +44 1225 383694.

E-mail address: F.Marken@bath.ac.uk (F. Marken).

was taken from a Thermo Scientific water purification system (Barnstead Nanopure) with not less than 18.2 MΩ cm resistivity. Experiments were conducted at 20 ± 2 °C. Argon gas (BOC, UK) was employed for de-aeration of the electrolyte solutions.

2.2. Instrumentation

Electrochemical experiments were conducted with a PGSTAT 12 Autolab system (Eco Chemie, Netherlands). The morphology of Fe(BTC) powder (as received), mechanically adhered on the electrode surface before and after the electrochemical reaction was characterized by scanning electron microscopy (SEM) with a JEOL JSM6480LV system.

2.3. Procedure for electrochemical measurements

All measurements were carried out in aqueous solution. A platinum wire and a saturated calomel electrode were used as counter and reference electrode, respectively. Working electrodes were 1.6 mm diameter platinum (BAS) or 4.9 mm diameter basal plane pyrolytic graphite electrode (Pyrocarbon, Le Carbone). For each experiment working electrodes were polished on SiC paper (1200 grit). MOF crystals were placed on clean Whatman 1 filter paper and gently transferred to the working electrode surface by rubbing the microcrystal powder into the graphite electrode surface [23].

3. Results and discussion

3.1. Voltammetric characterisation of Fe(BTC) in aqueous electrolyte media I: cation effects and reductive dissolution processes

Solid microcrystalline Fe(BTC) immobilised at the surface of basal plane pyrolytic graphite or at a platinum electrode and immersed into aqueous 0.1 M KCl shows no significant voltammetric response (not shown). This is in contrast to experiments with the well-known coordination polymer Prussian blue where well-defined electron transfer processes with coupled K⁺ insertion/expulsion [24] as well as structural changes [25] are observed. However, when adding acid into the aqueous electrolyte, the Fe(III/II) redox system for solid Fe(BTC) does appear. Fig. 1A shows the cyclic voltammograms obtained at a modified platinum electrode immersed in 0.1 M, 0.2 M, and 0.5 M HCl. The reduction and re-oxidation of Fe(III/II) are clearly observed as a reversible process with $E_{\text{mid}} = 0.48$ V vs. SCE. Interestingly, the midpoint potential for this voltammetric response is independent of the HCl concentration and therefore unlikely to be associated with proton insertion into the Fe(BTC) lattice. The mechanism is more likely due to a reductive dissolution (*vide infra*) similar to that observed for Cu₃(BTC)₂ system [26].

Cyclic voltammograms obtained under the same conditions but for Fe(BTC) immobilised at the surface of a basal plane pyrolytic graphite electrode (see Fig. 1B) show considerably less reactivity and a wider peak-to-peak separation. Only in aqueous 2 M HCl can the voltammetric response be clearly identified. Graphite surfaces are known to show slower rates of electron transfer (compared to platinum) towards Fe^{3+/2+} [27] and towards iron-containing minerals [28] and it is likely that here also the rate of electron transfer locally from graphite to the immobilised Fe(BTC) microcrystals is the key limiting parameter. On graphite the electron transfer process becomes potential driven and the peak-to-peak separation is considerably wider.

Fig. 1C demonstrates that the cyclic voltammetric response for Fe(BTC) immobilised onto platinum and immersed into 0.5 M HCl is highly reversible and stable over many potential cycles. The investigation of the effect of the potential scan rate on the peak currents for reduction and oxidation shows unusual “steady state” behaviour with essentially no change in peak current over a range of scan rates from 0.01 to 0.15 V s⁻¹ (note that the capacitive background current changes but not the Faradaic response). This type of characteristic can be attributed to a purely kinetically limited process (CE-type) where the slow dissolution

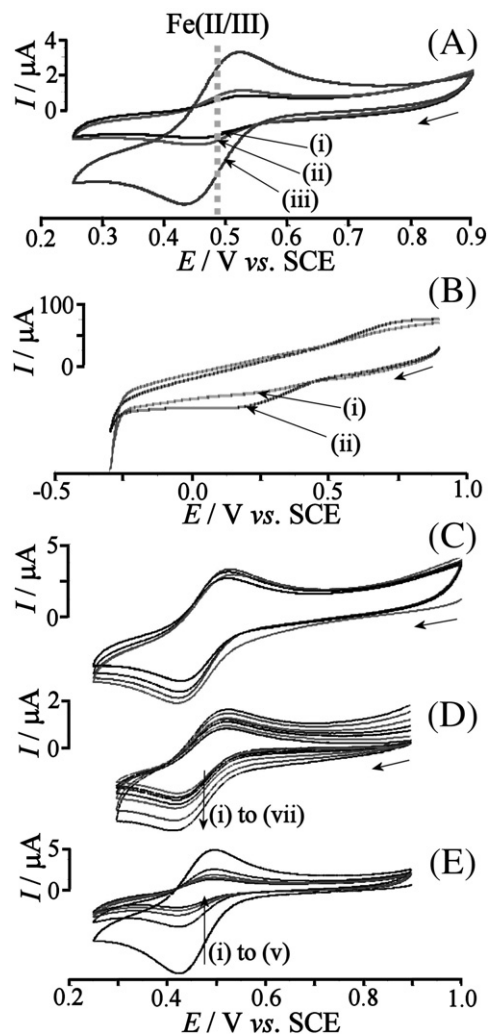
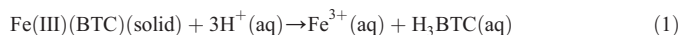


Fig. 1. (A) Cyclic voltammograms (scan rate 0.05 V s⁻¹) for the reduction of Fe(BTC) immobilised at the surface of a 1.6 mm diameter platinum disk electrode and immersed in aqueous (i) 0.1 M, (ii) 0.2 M, and (iii) 0.5 M HCl. (B) As above, but for a 4.9 mm basal plane pyrolytic graphite electrode (i) without and (ii) with Fe(BTC) immobilised and immersed in aqueous 2 M HCl. (C) Cyclic voltammograms (scan rate 0.05 V s⁻¹, 1st, 5th, 10th, and 20th potential cycles shown) for the reduction of Fe(BTC) immobilised at the surface of a 1.6 mm diameter platinum disk electrode and immersed in aqueous 0.5 M HCl. (D) As above with scan rates (i) 0.01 (ii) 0.02 (iii) 0.03 (iv) 0.04 (v) 0.05 (vi) 0.10 and (vii) 0.15 V s⁻¹. (E) As above (potential cycles 1 to 5 shown in (i) to (v)) but immersed in aqueous 2 M HCl.

of Fe³⁺ is limiting the current response. This conclusion is confirmed when experiments are conducted in 1 M and in 2 M HCl (see Fig. 1E). Now, the reductive dissolution and loss of electrochemically active material is clearly occurring at the electrode surface.

In order to investigate the conditions at the electrode surface further, scanning electron micrographs (SEMs) were obtained. Fig. 2A shows the microcrystalline Fe(BTC) powder sample with typical crystal sizes of 0.2 μm. After immobilisation at the platinum electrode surface the adhered microcrystalline material is clearly observed (see Fig. 2B).

The mechanism for the Fe-BTC reduction can be expressed (very over-simplified) as a reductive dissolution (see Eqs. (1) and (2)).



There are several possible intermediate species with BTC or chloride bound to the free Fe(III) species. The location for the process

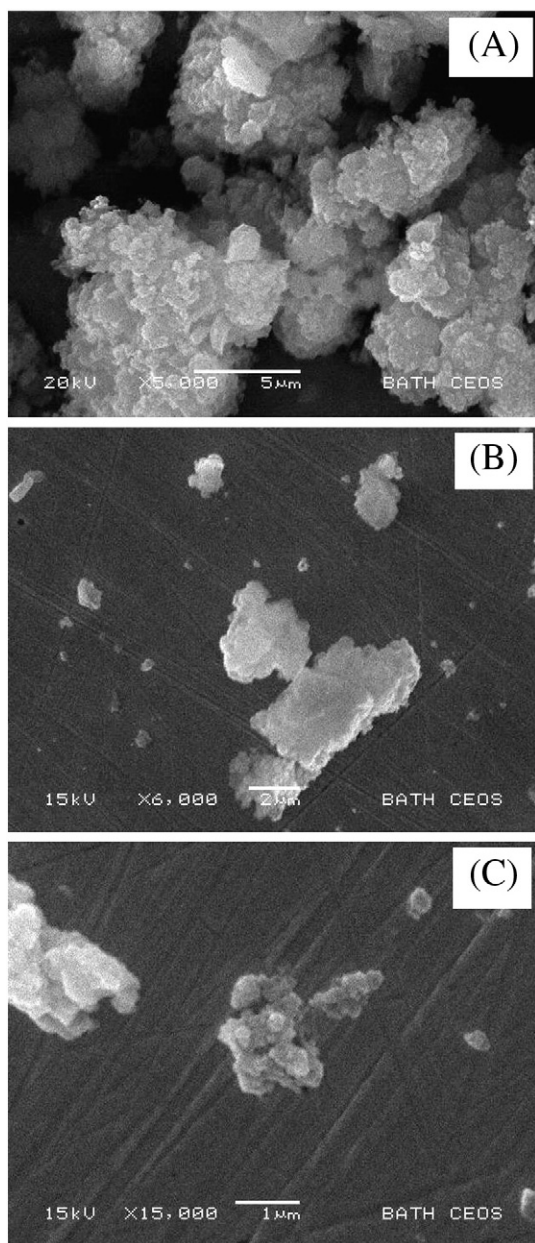


Fig. 2. SEM images of (A) Fe(BTC) bulk powder, (B) Fe(BTC) immobilised at a platinum disk electrode surface before and (C) after electrocatalytic hydroxide oxidation (see text).

at lower acid concentrations could be in close vicinity of the microcrystalline deposit and/or at the surface of the microcrystalline material with surface diffusion.

3.2. Voltammetric characterisation of Fe(BTC) in aqueous electrolyte media II: anion effects and electrocatalytic processes

It is of interest to explore potential electrocatalysis applications of novel porous materials and to rationalise electrocatalytic processes of solids immobilised at electrode surfaces. Prussian blues have found a wide range of applications based on electrocatalytic reactions [29].

First the effect of the supporting electrolyte anion is investigated. Fig. 3A shows cyclic voltammograms obtained in aqueous 0.5 M HNO₃ and in 0.5 M HCl. The chloride anion can be seen to somewhat enhance the voltammetric response which is consistent with the formation of intermediate iron chloride complexes during dissolution of Fe(III)(BTC).

Next the effect of hydroxide on the voltammetric responses for Fe(BTC) are investigated. A well-defined hydroxide oxidation response is observed when NaOH is added into a background electrolyte of aqueous 0.1 M KCl. Fig. 3B shows that oxidation peaks are observed at both Fe(BTC) modified platinum and basal plane pyrolytic graphite electrode surfaces. Fig. 3C shows that the oxidation peak is directly proportional to the hydroxide concentration and therefore diffusion controlled. The process is accompanied by the evolution of oxygen. The analysis of the slope of the plot (see inset in Fig. 3C) based on the appropriate Randles–Sevcik equation (see Eq. (3) [30]) allows the

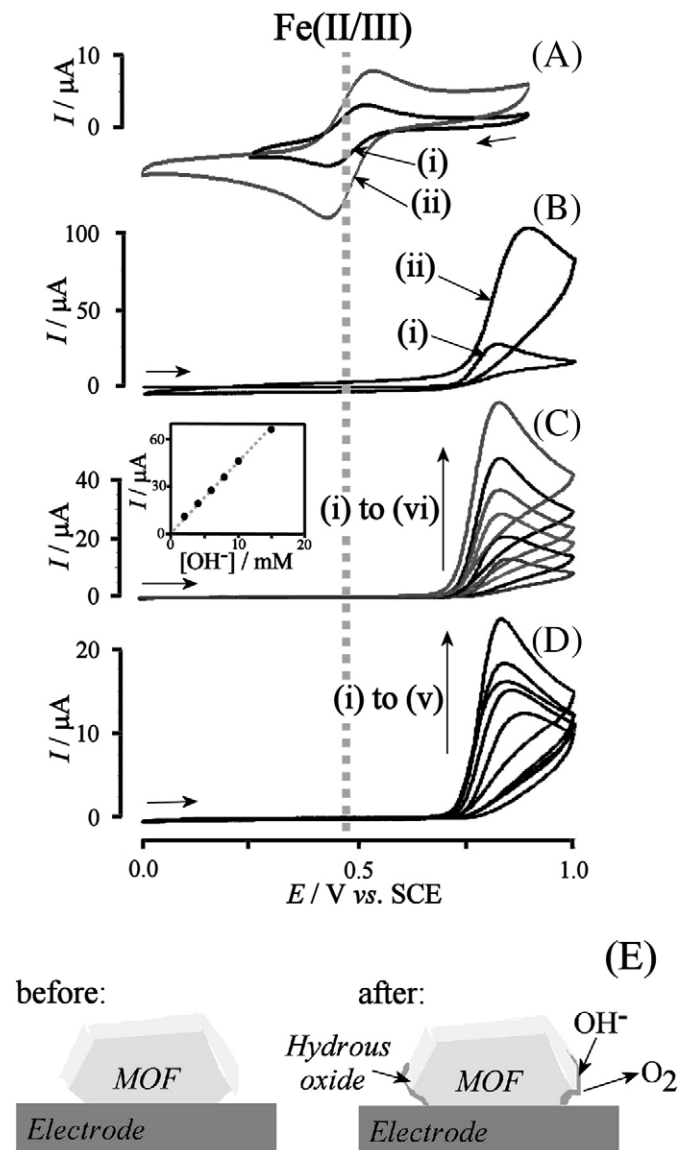


Fig. 3. (A) Cyclic voltammograms (scan rate 0.05 V s⁻¹) for the reduction of Fe(BTC) immobilised at the surface of a 1.6 mm diameter platinum disk electrode and immersed in aqueous (i) 0.1 M HNO₃ and (ii) 0.1 M HCl. (B) Cyclic voltammograms (scan rate 0.05 V s⁻¹) for the reduction of Fe(BTC) immobilised at the surface of (i) a 1.6 mm diameter platinum disk electrode and (ii) a 4.9 mm diameter basal plane pyrolytic graphite electrode immersed in aqueous 0.1 M KCl with 5 mM NaOH. (C) Cyclic voltammograms (scan rate 0.05 V s⁻¹) for the reduction of Fe(BTC) immobilised at the surface of a 1.6 mm diameter platinum disk electrode immersed in aqueous 0.1 M KCl with (i) 2, (ii) 4, (iii) 6, (iv) 8, (v) 10, and (vi) 15 mM NaOH (inset shows plot of peak current versus hydroxide concentration). (D) Cyclic voltammograms (scan rate 0.05 V s⁻¹, start potential (i) 0.5, (ii) 0.4, (iii) 0.3, (iv) 0.1, and (v) 0.0 V vs. SCE) for the reduction of Fe(BTC) immobilised at the surface of a 1.6 mm diameter platinum disk electrode immersed in aqueous 0.1 M KCl with 5 mM NaOH. (E) Schematic drawing of MOF attached to the working electrode surface before and after reductive catalyst formation.

approximate number of electrons n transferred per hydroxide diffusing to the electrode surface to be estimated.

$$I_p = 0.496nFAc\sqrt{\frac{nFvD}{RT}} \quad (3)$$

In this expression I_p is the anodic peak current, F is the Faraday constant, A is the geometric electrode area, c is the bulk hydroxide concentration, v is the scan rate, D is the hydroxide diffusion coefficient (here assumed to be $4.4 \times 10^{-9} \text{ m}^2 \text{ s}^{-1}$ [31]), R is the gas constant, and T is the absolute temperature. The value for $n=0.63$ calculated based on Eq. (3) and on data in Fig. 3C may appear low (a value between one and two is expected but partial blocking and uneven coverage have to be taken into account) but it suggests nearly one electron transferred per hydroxide in agreement with results obtained for hydrous iron oxide nanoparticle catalyst under similar conditions [32]. The formation of intermediate peroxide products is unlikely due to their reactivity in the presence of Fe(III) and therefore formation of O_2 appears most likely.

Closer inspection of the voltammetric behaviour reveals that Fe(BTC) is not immediately electrocatalytically active. Fe(BTC) modified platinum electrodes with the potential cycled between 0.6 and 1.0 V vs. SCE do not exhibit catalytic activity for the oxidation of hydroxide. However, upon applying a potential lower than 0.5 V vs. SCE the hydroxide oxidation process commences (see Fig. 3D). This “activation potential” for the Fe(BTC) catalyst is consistent with that for the Fe(III/II) reductive dissolution process under acidic conditions (vide supra), and therefore with the formation of hydrous iron oxide intermediates. Dissolution of Fe(III/II) under these alkaline conditions is unlikely and a mechanism based on Fe(BTC) surface modification appears plausible. SEM images of the Fe(BTC) catalyst immobilised at the platinum electrode surface before (Fig. 2B) and after (Fig. 2C) use for electrocatalytic hydroxide oxidation show no new deposits. Therefore a surface transformation of the Fe(BTC) microcrystalline material is proposed to explain the observed electro-catalytic reactivity (see Fig. 3E).

Further work will be required to compare and evaluate the reactivity of Fe(BTC) as oxygen evolution catalyst precursor, to explore the effect of the MOF precursor on the electrocatalytic process, and to identify further electrocatalytic processes possible with Fe(BTC) and similar designer MOF structures. In the future, structural modification of MOF systems to facilitate reversible electrochemical ion insertion and expulsion will be possible.

4. Summary

- (1) It has been shown that Fe(BTC) as a porous solid is electrochemically active in aqueous environments in the presence of protons and with platinum as the substrate electrode.
- (2) The Fe(III/II) redox process in aqueous acids is accompanied by a CE-type reductive dissolution process which at acid concentrations of 1 M or higher leads to rapid loss of Fe(BTC) from the electrode surface.
- (3) The complete absence of ion insertion processes (equivalent to those observed for Prussian blue) suggests a structural effect

impeding insertion. Most likely, the lack of binding sites for K^+ within the hydrophilic Fe(BTC) lattice is responsible for a kinetic barrier and/or thermodynamically unfavourable conditions (compare thermodynamic factors for ion insertion into Prussian blue [33]).

- (4) Fe(BTC) can be activated cathodically to act as an efficient oxygen evolution/water splitting electrocatalyst.

Acknowledgements

We are grateful for the support from the Royal Society for an International Joint Grant between University of Bath (UK) and Central Electrochemical Research Institute in Karaikudi (India).

References

- [1] A.U. Czaja, N. Trukhan, U. Müller, *Chem. Soc. Rev.* 38 (2009) 1284.
- [2] G. Férey, *Chem. Soc. Rev.* 37 (2008) 191.
- [3] M. Dinca, J.R. Long, *Angew. Chem. Int. Ed.* 47 (2008) 6766.
- [4] U. Mueller, M. Schubert, F. Teich, H. Puetter, K. Schierle-Arndt, J. Pastre, *J. Mater. Chem.* 16 (2006) 626.
- [5] S. Kitagawa, R. Kitaura, S. Noro, *Angew. Chem., Int. Ed.* 43 (2004) 2334.
- [6] J.L.C. Rowsell, O.M. Yaghi, *Microporous Mesoporous Mater.* 73 (2004) 3.
- [7] A.D. Burrows, C.G. Frost, M.F. Mahon, C. Richardson, *Angew. Chem., Int. Ed.* 47 (2008) 8482.
- [8] Z. Wang, S.M. Cohen, *Chem. Soc. Rev.* 38 (2009) 1315.
- [9] A.D. Burrows, C.G. Frost, M.F. Mahon, C. Richardson, *Chem. Commun.* (2009) 4218.
- [10] W. Lin, W.J. Rieter, K.M.L. Taylor, *Angew. Chem. Int. Ed.* 48 (2009) 650.
- [11] A. Doménech-Carbó, *Electrochemistry of porous materials*, CRC Press, London, 2010 p. 95.
- [12] A. Doménech, H. Garcia, M.T. Doménech-Carbo, F. Llabres-I-Xamena, *J. Phys. Chem. C* 111 (2007) 13701.
- [13] A. Doménech, H. Garcia, M.T. Doménech-Carbo, F. Llabres-I-Xamena, *Electrochem. Commun.* 8 (2006) 1830.
- [14] H. Lin, X. Wang, H. Hu, B. Chen, G. Li, *Solid State Sci.* 11 (2009) 643.
- [15] L.M. Rodriguez-Albelo, A.R. Ruiz-Salvador, A. Sampieri, D.W. Lewis, A. Gómez, B. Nohra, P. Mialane, J. Marrot, F. Sécheresse, C. Mellot-Draznieks, R.N. Biboum, B. Keita, L. Nadjo, A. Dolbecq, *J. Am. Chem. Soc.* 131 (2009) 16078.
- [16] K. Itaya, I. Uchida, V.D. Neff, *Acc. Chem. Res.* 19 (1986) 162.
- [17] R.J. Mortimer, *Chem. Soc. Rev.* 26 (1997) 147.
- [18] H.K. Chae, D.Y. Siberio-Perez, J. Kim, Y.B. Go, M. Eddaoudi, A.J. Matzger, M. O’Keeffe, O.M. Yaghi, *Nature* 427 (2004) 523.
- [19] M. Riou-Cavellec, G. Férey, *Solid State Sci.* 4 (2002) 1221.
- [20] L.H. Xie, S.X. Liu, C.Y. Gao, R.G. Cao, J.F. Cao, C.Y. Sun, Z.M. Su, *Inorg. Chem.* 46 (2007) 7782.
- [21] M. Riou-Cavellec, C. Lesaint, M. Nogues, J.M. Greneche, G. Férey, *Inorg. Chem.* 42 (2003) 5669.
- [22] R. Koncki, *Crit. Rev. Anal. Chem.* 32 (2002) 79.
- [23] F. Marken, S. Cromie, V. McKee, *J. Solid State Electrochem.* 7 (2003) 141.
- [24] R.C. Millward, C.E. Madden, I. Sutherland, R.J. Mortimer, S. Fletcher, F. Marken, *Chem. Commun.* (2001) 1994.
- [25] F. Scholz, U. Schröder, R. Gulaboski, *Electrochemistry of Immobilized Particles and Droplets*, Springer, 2005 p. 124.
- [26] A. Doménech-Carbó, *Electrochemistry of Porous Materials*, CRC Press, London, 2010 p. 98.
- [27] C.A. Frysz, X.P. Shui, D.D.L. Chung, *Carbon* 35 (1997) 893.
- [28] F. Scholz, B. Meyer, *Electroanal. Chem.* 20 (1998) 1.
- [29] N.R. de Tacconi, K. Rajeshwar, R.O. Lezna, *Chem. Mater.* 15 (2003) 3046.
- [30] F. Marken, A. Neudeck, A.M. Bond, in: F. Scholz (Ed.), *Electroanalytical Methods*, Springer, Berlin, 2002, p. 8.
- [31] R.N. Adams, *Electrochemistry at Solid Electrodes*, Marcel Dekker, New York, 1969, p. 221.
- [32] K.J. McKenzie, D. Asogan, F. Marken, *Electrochem. Commun.* 4 (2002) 820.
- [33] D.R. Rosseinsky, L. Glasser, H.D. Brooke Jenkins, *J. Am. Chem. Soc.* 126 (2004) 10472.